

Branched polymers on the Given-Mandelbrot family of fractals

Deepak Dhar

Department of Theoretical Physics, Tata Institute of Fundamental Research, Homi Bhabha Road, Mumbai 400 005, India

(Received 11 October 2004; published 11 March 2005)

We study the average number \bar{A}_n per site of the number of different configurations of a branched polymer of n bonds on the Given-Mandelbrot family of fractals using exact real-space renormalization. Different members of the family are characterized by an integer parameter b , $2 \leq b \leq \infty$. The fractal dimension varies from $\log_2 3$ to 2 as b is varied from 2 to ∞ . We find that for all $b \geq 3$, \bar{A}_n varies as $\lambda^n \exp(bn^\psi)$, where λ and b are some constants, and $0 < \psi < 1$. We determine the exponent ψ , and the size exponent ν (average diameter of polymer varies as n^ν), exactly for all b , $3 \leq b \leq \infty$. This generalizes the earlier results of Knezevic and Vannimenus for $b=3$ [Phys. Rev B **35**, 4988 (1987)].

DOI: 10.1103/PhysRevE.71.031801

PACS number(s): 61.25.Hq, 82.35.Lr, 05.45.Df

I. INTRODUCTION

The study of statistical physics models on deterministic fractals has a long history [1–4]. Linear and branched polymers on fractals with a finite ramification number provide very simple and pedagogical examples of renormalization group techniques at work: these systems show a nontrivial critical point, and the values of the critical exponents can be determined by linearizing the exact real-space renormalization transformation. The renormalization equations are coupled polynomial recursion equations in a finite number of variables, and are easy to study. By studying different geometrical fractals, one can investigate how the critical exponents change with the geometrical properties of the underlying space.

One particular family of fractals which has been used often for such studies is the Given-Mandelbrot family of fractals [5]. Different members of the family are characterized by an integer b , with $2 \leq b \leq \infty$. As we increase b from 2 to ∞ , the fractal dimension increases from $\log_2 3$ to 2. The critical properties of linear polymers on the $b=2$ fractal were studied in Ref. [2], and these results were extended to $b \leq 8$ by Elezovic *et al.* [6] using the exact renormalization equations. Surprisingly, it was found that while the exponent ν_b appeared to converge to the two-dimensional value $3/4$, as b was increased from 2 to 8, the difference in the susceptibility exponent γ_b from the known exact value $43/32$ in two dimensions was found to increase with increasing b . This was explained in Ref. [7], where the asymptotic behavior of critical exponents for large b was determined theoretically using finite-size scaling arguments, and it was shown that γ_b should tend to a different value $133/32$ for large b . Numerical Monte Carlo renormalization group techniques have been used to estimate the critical exponents for significantly larger values of b up to 80 [8,9]. Knezevic and Vannimenus (KV) used the real-space renormalization technique to study the properties of branched polymers on the $b=2$ fractal, and also studied the transition from the extended phase to collapsed phase [10]. This was later extended to other fractals, including the $b=3$ fractal [11]. Dense branched polymers for the $b=2$ fractal have been studied in the context of spanning trees and loop-erased random walks [12], and the Abelian sandpile model [13]. However, a study of branched polymers

on fractals for higher b has not been undertaken so far. Nor are the properties of the large- b limit known.

In this paper we study the number of different configurations of an n -bond branched polymer on the Given-Mandelbrot family of fractals using the exact real-space renormalization group techniques. On regular lattices, this number usually varies as $\lambda^n n^{-\theta}$, where λ is some lattice-dependent constant, and θ is a critical exponent. General theoretical arguments that prove the exponential growth would allow stronger correction terms like $\exp(bn^\psi)$, with $\psi < 1$. Why the first correction term to the exponential growth is a simple power-law term is not fully understood. To see how general is the power-law correction form, one can study this question on different graphs, e.g., fractals. We find the power-law correction also on the $b=2$ fractal. However, this case is exceptional. For all $b \neq 2$, while the number of configurations still increases exponentially with n , the leading correction term to the exponential growth is the stretched-exponential form: this number varies as $\lambda^n e^{bn^\psi}$, where λ and b are some constants, and $0 < \psi < 1$. We determine the singularity exponent ψ , and the size exponent ν (average diameter of polymer varies as n^ν), exactly for all b , $3 \leq b \leq \infty$. This generalizes the earlier results of KV for $b=2$ and 3.

This paper is organized as follows: In Sec. II, we start by recapitulating the definition of the Given-Mandelbrot family of fractals, and introduce the generating function for the number of branched polymer configurations with n monomers. Since the fractal does not have translational invariance, we average over different positions of the polymer. The general technique of real-space renormalization applied to these problems is outlined in Sec. III, using the $b=2$ case as an illustrative example. The qualitative behavior of the renormalization equations for $b \geq 3$ is discussed in Sec. IV. It turns out that while the equations involve rather complicated high-degree polynomials, the critical exponents ν and ψ do not depend on most of the terms in these polynomials. We can ignore most of these terms, and still determine the *exact* values of these exponents, if we can identify the “dominant terms” in the recursion equations. This is done in Sec. V. Finally, in Sec. VI, using our knowledge of the dominant terms, we determine the exponents ν and ψ for all $b \geq 3$,

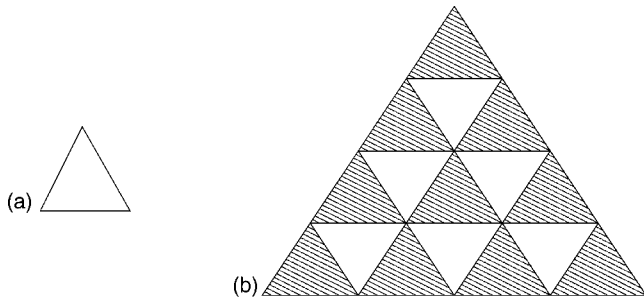


FIG. 1. The recursive construction of the Given-Mandelbrot fractal for $b=4$. (a) The graph of first-order triangle. (b) The graph of a $(r+1)$ -order triangle, formed by joining $b(b+1)/2$ r th-order triangles shown as shaded triangles here.

without having to write down the full set of recursion equations.

II. DEFINITIONS

For any given integer b , $2 \leq b < \infty$, the recursive construction of the Given-Mandelbrot family of fractals is shown in Fig. 1. We start with a graph with three vertices and three edges forming a triangle. This is called the first-order triangle. To construct the graph of the $(r+1)$ th-order triangle, we take graphs of $b(b+1)/2$ triangles of r th order, and glue them together (i.e., identify corner vertices) as shown in the figure, to form an equilateral triangle with base which is b times longer. The case $b=2$ corresponds to the well-known Sierpinski gasket (Fig. 2).

It is easy to see that the number of edges in the graph of the r th-order triangle is $3b^r(b+1)2^{-r}$, and all vertices have coordination number 4 or 6, except the corner vertices. The distance between the corner vertices of r th-order triangle is b^{r-1} . Thus the fractal dimension of the graph is $D_b = \log_b[b(b+1)/2]$. For $b=2, 3, 4, \dots$, these values are 1.5849, 1.6309, 1.6609, ..., respectively. For large b , the fractal dimension tends to 2 as $D_b \approx 2 - \log_b 2$. The spectral dimension \tilde{D}_b of the graph can also be calculated exactly for general b [14]. The values of \tilde{D}_b for $b=2-10$ are listed in Ref. [15]. For large b , \tilde{D}_b tends to 2, and the leading correction to its limiting value is given by $\tilde{D}_b \approx 2 - \log \log b / \log b$ [16].

The determination of the generating function for the branched polymers on these fractals follows the treatment of

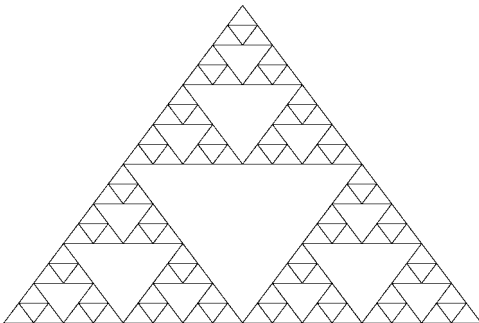


FIG. 2. The graph of a fifth-order triangle for $b=2$.

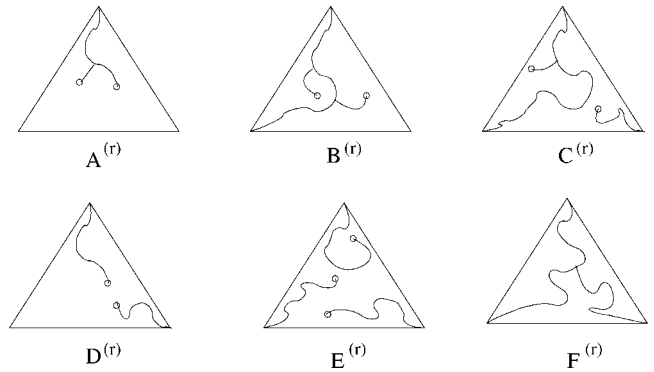


FIG. 3. Definition of the restricted partition functions $A^{(r)}$, $B^{(r)}$, $C^{(r)}$, $D^{(r)}$, $E^{(r)}$, and $F^{(r)}$.

Refs. [2,10,11]. Let $A_n(N)$ be the number of distinct single connected clusters of n bonds on a graph with N total number of bonds in the graph, different translations of the cluster being counted as distinct. For large N , this number increases linearly with N . We then define

$$\bar{A}_n = \lim_{N \rightarrow \infty} A_n(N)/N; \quad (1)$$

and

$$G(x) = \sum_{n=0}^{\infty} \bar{A}_n x^n, \quad (2)$$

where we assume the convention $\bar{A}_0 = 1$.

III. RENORMALIZATION EQUATIONS FOR THE $b=2$ FRACTAL

We assign a weight x^n to each configuration of the polymer with n occupied bonds, and define restricted partition functions $A^{(r)}$, $B^{(r)}$, $C^{(r)}$, $D^{(r)}$, $E^{(r)}$, and $F^{(r)}$, as shown in Fig. 3. Here $A^{(r)}$ is the sum of weights of all connected configurations of the branched polymer inside a r th-order triangle, such that only one of the corner vertices is occupied by the polymer, and the other two corner vertices are unoccupied. $D^{(r)}$ is the sum of weights of all configurations with two mutually disconnected clusters, each cluster connected to a specified corner vertex. $B^{(r)}$ consists of the sum of all configurations of polymer that connect two specified corner vertices of the triangle, with the third vertex remaining unoccupied. Similarly, $E^{(r)}$ and $F^{(r)}$ correspond to sums over all configurations with all three corner vertices occupied, mutually disconnected, and connected, respectively. $C^{(r)}$ corresponds to all three corner vertices occupied, but only two specified vertices connected to each other by paths involving occupied bonds lying within the triangle.

The values of these restricted functions for $r=1$ are

$$A^{(1)} = D^{(1)} = E^{(1)} = 1; \quad B^{(1)} = C^{(1)} = x; \quad F^{(1)} = 3x^2 + x^3. \quad (3)$$

It is straightforward to write down the recursion equations for these restricted partition functions at level $(r+1)$ in terms of those at level r . One has to sum over all possible polymer configurations for different r th-order triangles, subject to the constraint that all occupied bonds are connected to one of the

corner vertices of the $(r+1)$ th-order triangle. For example, for $b=2$, KV obtained

$$A^{(r+1)} = A[1 + 2B + 2B^2] + 2B^2C + F[B^2 + A^2 + 2BD], \quad (4)$$

$$B^{(r+1)} = B^2 + B^3 + F[4BC + 2AB] + F^2[B + D], \quad (5)$$

$$C^{(r+1)} = AB^2 + 3B^2C + F[7C^2 + 2BD] + F^2[C + E], \quad (6)$$

$$D^{(r+1)} = A^2 + B[6C^2 + 4AC + 2A^2] + D[2B + 3B^2] + 2F[2CD + AD + BC + BE], \quad (7)$$

$$E^{(r+1)} = A^3 + 14C^3 + 12BCD + 6ABD + 3B^2E + 3F[C^2 + D^2 + 4CE], \quad (8)$$

$$F^{(r+1)} = 3FB^2 + 6F^2C + F^3, \quad (9)$$

where we have dropped the superscript (r) over all the variables in the right-hand side of all the recursion equations to simplify notation. The generating function $G(x)$ is expressible in terms of these variables,

$$G(x) = \sum_{r=1}^{\infty} 3^{-r} (A^{(r)2} + A^{(r)2}B^{(r)} + B^{(r)2}D^{(r)}). \quad (10)$$

It was shown by KV that there exists a critical value x_c , such that for all $x < x_c$, $(A^{(r)}, B^{(r)}, C^{(r)}, D^{(r)}, E^{(r)}, F^{(r)})$ tends to a fixed point $(A^*(x), 0, 0, A^{*2}(x), A^{*3}(x), 0)$, where the value of $A^*(x)$ increases monotonically from 1 to ∞ as x increases from 0 to x_c . For all $x > x_c$, $A^{(r)}, B^{(r)}, C^{(r)}, D^{(r)}, E^{(r)}, F^{(r)}$ all diverge to infinity. At $x = x_c$, the values of $A^{(r)}, C^{(r)}, D^{(r)}$, and $E^{(r)}$ diverge to infinity for large r . If we change variables to $\tilde{A} = AF, \tilde{B} = B, \tilde{C} = CF, \tilde{D} = DF^2$, and $\tilde{E} = EF^3, \tilde{F} = F$, the non-trivial fixed point occurs at finite values of $\tilde{A}, \tilde{B}, \tilde{C}, \tilde{D}, \tilde{E}$, with $\tilde{F} = 0$. Linearized analysis of the renormalization equations near the fixed point determines the singularity exponent θ for the function $G(x) \sim |x_c - x|^{\theta-1}$, and the exponent ν (correlation length $\sim |x_c - x|^{-\nu}$). KV found $\nu = 0.71655$ and $\theta = 0.5328$.

IV. RENORMALIZATION EQUATIONS FOR $b \geq 3$

Interestingly, the qualitative behavior of the recursion equations is very different for $b > 2$. For $b=3$, the singularity of $G(x)$ is not a power-law singularity, but an essential singularity [11]. The case $b > 3$ has not been studied so far.

For a general value of b , the equations are still coupled polynomial recursion equations in six variables. We denote the six functions $A^{(r)}, B^{(r)}, \dots, F^{(r)}$ by $K_i^{(r)}$, with $i=1-6$, and represent the polynomial recursion equations schematically as

$$K_i^{(r+1)} = f_i(\{K_j^{(r)}\}), \quad \text{for } i=1-6, \quad (11)$$

where f_i are some (b -dependent) polynomial functions of their six arguments. One can also write the generating func-

tion $G(x)$ in terms of $\{K_i^{(r)}\}$ in a polynomial form similar to Eq. (10),

$$G(x) = \sum_{r=1}^{\infty} [b(b+1)/2]^{-r} g(\{K_j^{(r)}\}). \quad (12)$$

It is rather tedious to write down the explicit forms of these polynomials for any $b > 3$. The number of terms in each f_i increases very fast with b . There are approximately 100 terms in each of the recursion equations for $b=3$ [17], and the number would run into thousands for $b=4$. The number of terms would increase as b^{12} for large b , as that is the number of polynomials with six variables with maximum degree $b(b+1)/2$. Also, the coefficients of the terms become very large, increasing as $\exp(b^2)$. Even for $b=3$, to generate the recursion equations, one has to use a computer. It seems clear that a brute-force approach to determine the recursion equations is not feasible, except for a few additional values of b .

Interestingly, even though the recursion equations are rather complicated, we show below that for all $b \geq 3$, the generating function has an essential singularity of the type $G(x) \sim \exp(a|x_c - x|^{-\alpha})$. This corresponds to $A_n \sim x_c^{-n} \exp(bn^\psi)$, where b is some constant, and $\psi = \alpha/(1+\alpha)$. We determine the exact value of the b -dependent exponents ψ and ν for all b .

If we start with the initial conditions [Eq. (3)], and iterate the recursion equations, KV found that many qualitative features of the behavior of the recursion equations for the $b=3$ case are same as for $b=2$: for all x below a critical value x_c , $(A^{(r)}, B^{(r)}, C^{(r)}, D^{(r)}, E^{(r)}, F^{(r)})$ tends to a fixed point $(A^*(x), 0, 0, A^{*2}(x), A^{*3}(x), 0)$, where $A^*(x)$ diverges to infinity as x tends to x_c from below. For all $x > x_c$, the values of all $\{K_i\}$ tend to infinity for large r . For $x = x_c$, both for $b=2$ and 3, the values of $A^{(r)}, D^{(r)}$, and $E^{(r)}$ tend to infinity, while $C^{(r)}$ and $F^{(r)}$ decrease to zero with iteration. The main difference is the limiting behavior of $B^{(r)}$ at $x = x_c$. It tends to a nonzero limit for $b=2$, but to zero for $b=3$. Also, the variables $\{\ln K_i^{(r)}\}$ increase linearly with r for $b=2$, but they increase exponentially with r for $b=3$.

What makes this problem tractable is the fact that while the polynomial recursion equations are complicated, the asymptotic behavior of the variables depends only on a few terms in the recursion equations. To see this, consider first the simple case when each function f_i has only a single term, and is of the form

$$K_i^{(r+1)} = c_i \prod_{j=1}^6 [K_j^{(r)}]^{m_{ij}}, \quad (13)$$

where \mathbf{m} is 6×6 matrix of non-negative integers. These recursion equations reduce to linear recursions on taking logarithms of both sides. We get

$$\ln K_i^{(r+1)} = \sum_{j=1}^6 m_{ij} \ln K_j^{(r)} + \ln c_i. \quad (14)$$

These are easily solved. We get that for large r , the leading behavior of $K_i^{(r)}$ is given by

$$\ln K_i^{(r+1)} = \sum_{j=1}^6 \left[(\mathbf{m}^r)_{ij} \ln K_j^{(1)} + \left(\frac{\mathbf{m}^r - 1}{\mathbf{m} - 1} \right)_{ij} \ln c_j \right]. \quad (15)$$

Let the eigenvalues of the matrix \mathbf{m} be $\{\lambda_\alpha\}$, $\alpha=1-6$, ordered so that $\lambda_\alpha > \lambda_{\alpha+1}$. Let the corresponding right eigenvectors be $v_{i\alpha}$, so that

$$\mathbf{m}_{ij} v_{i\alpha} = \lambda_\alpha v_{i\alpha}. \quad (16)$$

Then, using the eigenvector decomposition of \mathbf{m} , we see that for large r

$$\ln K_i^{(r)} = \delta_1 \lambda_1^r v_{i1} + \delta_2 \lambda_2^r v_{i2} + \text{higher order terms}, \quad (17)$$

where δ_1 and δ_2 are some coefficients, that can be expressed in terms of $K_i^{(1)}$, c_j 's, and the left eigenvectors of \mathbf{m} . As \mathbf{m} has non-negative elements and $c_i \geq 1$, v_{i1} are of the same sign, which can be chosen positive. Then all K_i 's increase or decrease with iteration for large r according as $\delta_1 > 0$ or $\delta_1 < 0$. Thus $\delta_1 = 0$ must correspond to $x = x_c$, and for small deviations of x from x_c , by continuity, we will have δ_1 proportional to $(x - x_c)$.

If $\delta_1 = 0$, then the behavior of K_i 's for large r is governed by the second term in Eq. (17). In this case, all v_{i2} 's are not of same sign. If v_{12} , v_{42} , and v_{52} are positive, and the rest negative, we would get K_1 , K_4 , and K_5 to diverge, and K_2 , K_3 , and K_6 tend to zero for large r , as expected from the preceding discussion.

Conversely, consider the full recursion equation (11). For any two infinite sequences $a^{(r)}$ and $b^{(r)}$ whose logarithm diverges to infinity as r increases, we define the notation

$$a \cong b, \text{ iff } \lim_{r \rightarrow \infty} \frac{\ln a^{(r)}}{\ln b^{(r)}} = 1. \quad (18)$$

We make the ansatz that at $x = x_c$, for large r we have

$$K_i^{(r)} \cong \exp(v_i \lambda^r). \quad (19)$$

Then, as the number of terms in the recursion equations is finite, for each K_i , there must be at least one term in the right-hand side of its recursion equation for which the asymptotic rate of growth of the logarithm is exactly as the same as that of the left-hand side. We can define a matrix \mathbf{m} such that this dominant term is of the form of Eq. (13). Then we must have

$$\lambda v_i = \sum_{j=1}^6 \mathbf{m}_{ij} v_j, \quad (20)$$

while all other terms in the equation for K_i are either negligible for large r , or make a contribution of comparable amount. These dominant terms define the matrix \mathbf{m} . The vector $\{v_j\}$, then, is a right eigenvector of \mathbf{m} , with eigenvalue λ .

If there is more than one term that makes contributions of the same order, say in the recursion equation for K_i , then for any two such terms, there are two different row vectors \mathbf{m}_i and \mathbf{m}'_i that satisfy Eq. (20). Then we can subtract these to get a relation

$$\sum_{j=1}^6 [\mathbf{m}_{ij} - \mathbf{m}'_{ij}] v_j = 0. \quad (21)$$

There is one such equation for every such pair. However, all of them are not independent. We first reduce these to the minimal set of linearly independent equations. Then, each one of such equations can be used to eliminate one of the v 's, and then write Eq. (20) as an equation in fewer variables, with a new lower-dimensional matrix \mathbf{m} . This also changes the coefficients c_i and the eigenvectors, but does not change the value of λ_1 and λ_2 .

For example, for the $b=3$ fractal, KV found that the dominant terms in the recursion equations are

$$A' = 2A^2 B^2, \quad (22)$$

$$B' = A^2 B^2 F + 3AB^4, \quad (23)$$

$$C' = 3A^2 B^4 + A^3 B^2 F, \quad (24)$$

$$D' = 4A^3 B^2, \quad (25)$$

$$E' = 6A^4 B^2, \quad (26)$$

$$F' = 2B^6 + 6AB^4 F. \quad (27)$$

We note that the right-hand side involves only A , B , and F , and the variables C , D , and E can be determined in terms of these. In Eq. (23), the two terms on the right-hand side are of same order if and only if $AF \cong B^2$. This corresponds to the condition

$$v_1 - 2v_2 + v_6 = 0. \quad (28)$$

Note that we get the same condition if we had used Eqs. (24), or (27) instead of Eq. (23). Let

$$\lim_{r \rightarrow \infty} \frac{A^{(r)} F^{(r)}}{(B^{(r)})^2} = f^*. \quad (29)$$

Then we can write $F = f^* B^2 / A$ for large r , and eliminate F and work with a simpler set of recursions

$$A' = 2A^2 B^2, \quad B' = (3 + f^*) AB^4. \quad (30)$$

This corresponds to a 2×2 matrix,

$$\mathbf{m} = \begin{pmatrix} 2 & 2 \\ 1 & 4 \end{pmatrix}. \quad (31)$$

With this change of variables, the other equations also reduce to single term equations. Also, the matrix \mathbf{m} , and hence the eigenvalues λ_1 and λ_2 do not depend on the coefficient $(3 + f^*)$.

Similarly, in other cases, the asymptotic behavior of the variables K_i 's with the full complicated polynomial recursion relations may be reduced to that for a simpler system of equations where only one term (to be called the dominant term) is kept from each polynomial f_i in Eq. (11).

The dominant terms are not unique. Only a few terms in each of the polynomials $f_i(\{K_j\})$ are dominant, and any of them can be used for determining the matrix \mathbf{m} , and hence the eigenvalues λ_1 and λ_2 .

We note that in the neighborhood of different fixed points, different terms are dominant. For example, for branched

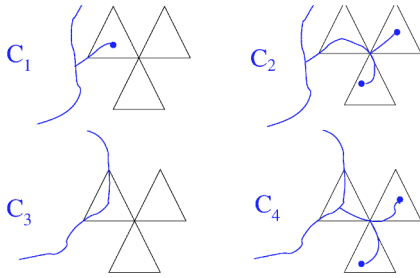


FIG. 4. Local modification of polymer configurations to increase its weight. The weight increases are going from configuration C_1 to C_2 , and from C_3 to C_4 .

polymers with attractive self-interaction, the fixed point corresponding to the dense phase is $\{K_{ij}\}=\{0,0,\infty,0,\infty,\infty\}$. Clearly, near this fixed point, the dominant terms are different.

V. IDENTIFYING THE DOMINANT TERMS

The problem of determining the critical exponents for our problem thus is reduced to that of identifying what are the dominant terms in the recursion equations. Each term in the recursion equation corresponds to a class of configurations of the polymers. However, all possible combinations of powers are not allowed in a given equation, as there are connectivity constraints on the allowed configurations. For example, a term like $E^{b(b+1)/2}$ corresponding to all r th-order triangles with configurations of type E has monomers not connected to the corners, and is not allowed.

Also, we note that while we may allow polymers with loops, the ratios like $F^{(r)}/C^{(r)}$ and $B^{(r)}/D^{(r)}$ tend to zero for large r . Thus any term corresponding to a polymer with loops is dominated by one without loop, obtained by removing one of the bonds in the loop (which changes a type F triangle into type C , or type B into type D). Thus loops are irrelevant, and the dominant terms correspond to polymer configurations without loops.

To understand the characteristics of dominant configurations better, it is instructive to look at configurations that differ from each other locally. Consider configurations C_1 and C_2 shown in Fig. 4. We assume that these are identical to each other, except in the three r th-order triangles shown. In C_1 , the vertex common to the three triangles shown is not connected to the polymer, but in C_2 it is. Then if C_1 is an allowed configuration, which is connected to the outside in a specified way, so is C_2 . If the weight of the rest of polymer outside the three triangles is \mathcal{W} , the weight of C_1 is $\mathcal{W}A$, while that of C_2 is $\mathcal{W}BA^2$. The ratio of weights is AB , which tends to infinity for large r (we shall show this later). This implies that a configuration of type C_2 will dominate over the corresponding C_1 .

Again, assume that C_3 and C_4 in Fig. 4 are the same configuration outside the three triangles shown. The ratio of weights of C_4 and C_3 is A^2F/B . This also tends to infinity for large r (also proved later), and hence given a configuration of type C_1 or C_3 , with two “empty” triangles near the polymer, we can attach a sidebranch to the polymer to create a configuration that dominates over it.

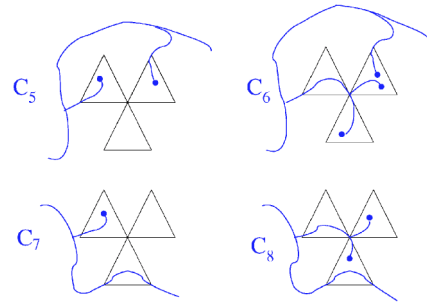


FIG. 5. Some examples of configurations where extending the polymer configuration is not favorable. Here C_5 has higher weight than C_6 , and C_7 has higher weight than C_8 .

This technique of creating a more dominant configuration by attaching sidebranches works only if the two triangles into which the polymer is extended are initially totally empty of polymer. This is shown in Fig. 5, where again we obtain the configuration C_6 by attaching more monomers to the polymer configuration C_5 , with configuration of polymer outside the triangles remaining unchanged. In this case, the ratio of weights of C_6 and C_5 is DB/A , which we shall show tends to zero or large r . Hence configurations of type C_5 dominate over C_6 . Similarly, we can see that ratio of weights of C_8 and C_7 is C , which tends to zero for large r . Thus a configuration like C_7 is dominant over the corresponding configuration of type C_8 . We see that C or D type vertices are not favored in creating a dominant configuration.

We can start with any allowed configuration of the polymer, and use this local modification to generate configurations which are more dominant (Fig. 6). If we start with an initial configuration with a small segment of polymer, with many empty triangles, we find growth at tips or sidebranches is favorable. We continue this until no such growth sites can be found, and any further growth of polymer reduces its weight. This is then the maximal weight configuration. Figure 7 shows two such configurations for the $b=7$ fractal corresponding to configurations of type A . We see that in a maximal weight configuration in a $(r+1)$ th-order triangle, the polymer goes through as many as possible of the corner vertices of the r th-order triangles that are *inside* the $(r+1)$ th-order triangle (not at the boundary of it), and do not contain any type C , D , or E vertices. This is a generalization of the observation of KV [11] that the dominant terms in the recursion equations had the central node of the triangle occupied.

To generate the different terms that are dominant for the different terms in different K_i , we can take the dominant configuration for $A^{(r+1)}$, and modify it appropriately. For ex-

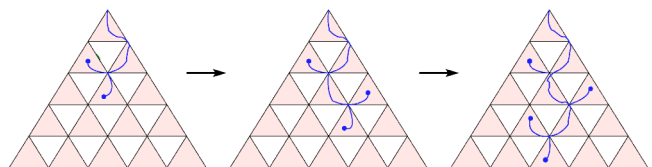


FIG. 6. Generating the dominant configuration by extending the cluster.

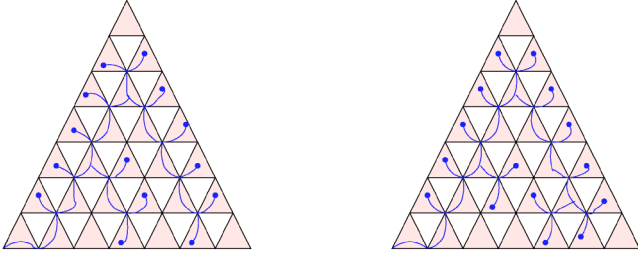


FIG. 7. Two of the dominant configurations that contribute to $A^{(r+1)}$ for the $b=7$ fractal.

ample, consider the dominant configurations for $B^{(r+1)}$. Now, in the dominant configuration for $A^{(r+1)}$, the polymer is as extended as possible, and hence will reach very close to the other corners of the $(r+1)$ th-order triangle. Then we have to make only a local modification in the triangles near this corner to connect it to the corner. This is shown in Fig. 8. Let the weight of the dominant configurations of $A^{(r+1)}$ be \mathcal{X} , and the multiplicative factor needed to convert its weight into that of $B^{(r+1)}$ be \mathcal{Y} .

Then, we have, by definition,

$$A^{(r+1)} \cong \mathcal{X}; B^{(r+1)} \cong \mathcal{X}\mathcal{Y}. \quad (32)$$

To get the dominant configuration of $F^{(r+1)}$, we have to connect the dominant polymer configuration of $A^{(r+1)}$ to both of the other corners. As the polymer in the dominant configuration reaches close to both of them, these local modifications can be done independently. Hence we get

$$F^{(r+1)} \cong \mathcal{X}\mathcal{Y}^2. \quad (33)$$

To get the dominant configurations for $D^{(r+1)}$, we have to add a polymer segment disconnected to the first to the second corner. This can also be done by a local modification of the configuration near the corner (see Fig. 8). We define \mathcal{Z} as the factor by which we have to multiply the weight of the configuration of $A^{(r+1)}$ to affect this change. Thus we have

$$D^{(r+1)} \cong \mathcal{X}\mathcal{Z}. \quad (34)$$

Dominant configurations for $E^{(r+1)}$ involve two such local changes, which can be done independently. Similarly, for $C^{(r+1)}$ also, we have to make local modifications at the two corners, connecting one corner to the existing $A^{(r+1)}$ cluster, and adding a disconnected cluster at the second corner. This gives us

$$E^{(r+1)} \cong \mathcal{X}\mathcal{Z}^2; C^{(r+1)} \cong \mathcal{X}\mathcal{Y}\mathcal{Z}. \quad (35)$$

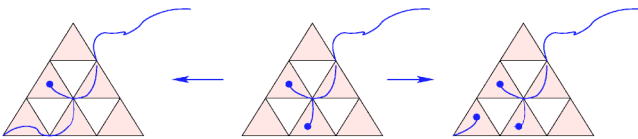


FIG. 8. Changing a dominant configuration for $A^{(r+1)}$ (middle figure) to one for $B^{(r+1)}$ (left figure) or $D^{(r+1)}$ (right figure) by local change near a corner. The polymer is connected to another corner vertex of the $(r+1)$ th-order triangle (not shown in figure).

Thus as far as the dominant terms are concerned, we can express the six functions f_i in terms of three functions \mathcal{X} , \mathcal{Y} , and \mathcal{Z} . Equivalently, we can eliminate three of the variables (say C , E , and F) using the relations

$$D^2 \cong AE, \quad B^2 \cong AF, \quad AC \cong BD. \quad (36)$$

We note that the weights of the two configurations shown in Fig. 7 are $A^{14}B^8F^2$ and $A^{15}B^6F^3$, respectively. If $B^2 \cong AF$, these make asymptotically equal contribution $A^{12}B^{12}$ to \mathcal{X} .

Also, as $A^2F/B \cong AB$, it follows that the weight increases by the same factor AB in going from configuration of type C_1 to C_2 , and from C_3 to C_4 (Fig. 4). Similarly, the weight changes by the same factor $BD/A \cong C$, when going from C_5 to C_6 , as in going from C_7 to C_8 . Again, as $C^{(r)}$ tends to zero for large r , we have justified the assumption made earlier about such extensions being unfavorable.

VI. CRITICAL EXPONENTS FOR $b \geq 3$

If we start with the shortest polymer class of configurations that contribute to $A^{(r+1)}$ having just weight $A^{(r)}$, then the first extension is by a corner vertex at the boundary of the triangle, and the resulting weight is AB . For any subsequent extension, using either extension of type $C_1 \rightarrow C_2$, or $C_3 \rightarrow C_4$, the weight increases by a factor AB . After n such extensions, the weight of the configuration is $A^n B^n$. For weight to be maximal, we want n to be as large as possible. It is easy to check that the largest value of n allowed (to be denoted by β here) is

$$\beta = (b^2 - 1)/4, \text{ if } b \text{ is odd,} \quad (37)$$

$$= b^2/4, \text{ if } b \text{ is even.} \quad (38)$$

For example, both configurations shown in Fig. 7 have $\beta=12$. From the argument given above, any further extension of the polymer will be unfavorable. Hence such configurations correspond to the maximal term. If the number of such configurations is $d(b)$, we have

$$\mathcal{X} = d(b)A^\beta B^\beta. \quad (39)$$

It is difficult to determine $d(b)$ explicitly for a general value of b . Of course, one can determine it for small b . This number would be expected to increase as $\exp(b^2)$ for large b . Fortunately, its precise numerical value does not matter for determining the exponents ν and ψ .

We can similarly determine \mathcal{Y} and \mathcal{Z} . To modify the dominant configuration of $A^{(r+1)}$ to that for $B^{(r+1)}$, one notes that as the former corresponds to a maximally extended polymer, one can find specific configurations such that the polymer reaches up to the r th-order triangle neighboring the corner which we want to reach. Then only changing the configuration in two such triangles is enough (Fig. 8). This gives us

$$\mathcal{Y} = B^2/A. \quad (40)$$

Similarly, to get configuration of type $D^{(r+1)}$ from \mathcal{X} , we need only add an A -type vertex at that corner (Fig. 8). This gives

$$\mathcal{Z} = A. \quad (41)$$

Putting all these together, we see that at the critical point, the recursion equations for $A^{(r)}$ and $B^{(r)}$ are given by

$$\begin{pmatrix} \ln A^{(r+1)} \\ \ln B^{(r+1)} \end{pmatrix} = \begin{pmatrix} \beta & \beta \\ \beta - 1 & \beta + 2 \end{pmatrix} \begin{pmatrix} \ln A^{(r)} \\ \ln B^{(r)} \end{pmatrix} + \begin{pmatrix} c_1 \\ c_2 \end{pmatrix}. \quad (42)$$

For the 2×2 matrix given above, the equation determining the eigenvalues is

$$\lambda^2 - 2(\beta + 1)\lambda + 3\beta = 0, \quad (43)$$

whose roots are

$$\lambda_{\pm} = \beta + 1 \pm \sqrt{\beta^2 - \beta + 1}. \quad (44)$$

If $\delta = x_c - x$ is very small, then it increases by a factor λ_+ under iteration, until it becomes sufficiently large so that linear analysis near the fixed point is no longer applicable. The number of iterations r_{max} required for the deviation to become $O(1)$ is given by

$$\lambda_+^{r_{max}} \delta \approx O(1) \quad (45)$$

whence we get

$$r_{max} = \ln(1/\delta) / \ln \lambda_+. \quad (46)$$

The linear size of polymer varies as $b^{r_{max}} \sim (1/\delta)^\nu$ with

$$1/\nu = \log_b \lambda_+. \quad (47)$$

It is easy to check that for large b , ν has an expansion of the form

$$1/\nu = D_b \left(1 - \frac{1}{b \ln(b^2/2)} + \text{higher order terms} \right). \quad (48)$$

For $\delta \ll 1$, $\ln A^{(r)}$ increases as λ_-^r . The maximum contribution to $G(x)$ in Eq. (12) comes from the term $r = r_{max}$, hence we can replace the sum by the largest term, and write $\ln G(x) \sim \ln \mathcal{X}^{(r_{max})} \sim \lambda_-^{r_{max}}$. This gives $\ln G(x) \sim (1/\delta)^{-a}$, with

$$a = \frac{\ln \lambda_-}{\ln \lambda_+}. \quad (49)$$

For large b , this varies as $\ln(3/2)/\ln b$, and tends to zero as b tends to infinity.

If $G(x)$ varies as $\exp[(x_c - x)^{-a}]$ for x near x_c , it is easy to see that coefficient of x^n in the Taylor expansion of $G(x)$ varies as $x_c^{-n} \exp(bn^a)$ where b is some constant, and $\psi = a/(1+a)$.

We have listed the numerical values of the critical exponents $1/\nu$ and ψ , along with the fractal dimension D_b for some representative values of b in Table I.

VII. DISCUSSION

The critical exponent ν does not tend to the two-dimensional value as b tends to infinity. This is not very

TABLE I. The fractal dimension D_b , and critical exponents $1/\nu$ and ψ for some values of b .

b	D_b	$1/\nu$	ψ
3	1.63093	1.41484	0.13250
4	1.66096	1.55263	0.13381
5	1.68261	1.57268	0.12429
7	1.71241	1.64448	0.10702
10	1.74036	1.70342	0.09154
15	1.76787	1.74406	0.07825
25	1.79685	1.78466	0.06568
50	1.82788	1.82292	0.05375
100	1.85165	1.84951	0.04543

surprising, and a similar behavior has been encountered before in the case of the susceptibility exponent for linear polymers. Basically, there is a crossover from the two-dimensional Euclidean value to the fractal value. For polymers with n monomers, with linear size $\ll b$ (i.e., $n \ll b^{1/\bar{\nu}}$, where $\bar{\nu}$ is the two-dimensional value), the space looks Euclidean, and their mean size will be similar to that of polymers in regular two-dimensional space. However, polymers with $n \gg b^{1/\bar{\nu}}$ feel the constrictions of the corners strongly, and try to avoid them, and become more compact. Their average size is given by n^ν , with critical exponent ν dependent on b . There is no exponent θ that we can define for any $b \geq 3$, because of the presence of the essential singularity.

One can define the chemical distance exponent z for our problem, just as we do for the Euclidean problem. We take two sites on the branched polymer at a distance ℓ as measured along bonds of the polymer. If the average Euclidean distance between these points is $\bar{r}(\ell)$, we define the exponent z by the relation $\bar{r}(\ell) \sim \ell^{1/z}$, for $1 \ll \ell \ll n^{1/\nu}$. We have not been able to calculate z for different values of b .

We note that the logarithm of the number of configurations of polymer acts like the entropy. The nontranslationally invariant fractal lattice provides a deterministic model for the inhomogeneous environment encountered by the polymer in a random environment. In this case, it would seem more reasonable to average the logarithm of the number of configurations of rooted branched polymers over different positions of the root, as that would correspond to averaging the free energy of the polymer over different positions of the polymer in space. Such averages have been calculated only very recently for linear polymers on fractals [18]. It would be interesting to see if the stretched exponential form for branched polymers is seen also in these ‘‘quenched’’ averages. Another open problem is the calculation of exponents characterizing the collapse transition of self-attracting polymers on these fractals. It is hoped that future works will throw some light on these questions.

- [1] D. R. Nelson and M. E. Fisher, *Ann. Phys. (N.Y.)* **91**, 226 (1975).
- [2] D. Dhar, *J. Math. Phys.* **18**, 577 (1977); **19**, 5 (1978).
- [3] Y. Gefen, B. B. Mandelbrot, and A. Aharony, *Phys. Rev. Lett.* **45**, 855 (1980).
- [4] R. Rammal, G. Toulouse, and J. Vannimenus, *J. Phys. (Paris)* **45**, 389 (1984).
- [5] J. A. Giam and B. B. Mandelbrot, *J. Phys. A* **16**, L565 (1983).
- [6] S. Elezovic, M. Knezevic, and S. Milosevic, *J. Phys. A* **20**, 1215 (1987).
- [7] D. Dhar, *J. Phys. (Paris)* **49**, 397 (1988).
- [8] S. Milosevic and I. Zivic, *J. Phys. A* **24**, L833 (1991).
- [9] I. Zivic and S. Milosevic, *J. Phys. A* **26**, 3393 (1993).
- [10] M. Knezevic and J. Vannimenus, *Phys. Rev. Lett.* **56**, 1591 (1986).
- [11] M. Knezevic and J. Vannimenus, *Phys. Rev. B* **35**, 4988 (1987).
- [12] D. Dhar and A. Dhar, *Phys. Rev. E* **55**, R2093 (1997).
- [13] F. Daerden, V. B. Priezhev, and C. Vanderzande, *Physica A* **292**, 43 (2001).
- [14] D. Dhar, *J. Phys. A* **21**, 2261 (1988).
- [15] R. Hilfer and A. Blumen, *J. Phys. A* **17**, L537 (1984).
- [16] S. Milosevic, D. Stassinopoulou, and H. E. Stanley, *J. Phys. A* **21**, 1477 (1988).
- [17] M. Knezevic, Ph.D. thesis, University of Paris VI, Paris, 1986.
- [18] Sumedha and D. Dhar (unpublished).